Signal Processing 92 (2012) 19–28

Contents lists available at ScienceDirect

Signal Processing

journal homepage: www.elsevier.com/locate/sigpro

Two-dimensional DOA estimation of coherent signals using acoustic vector sensor array

P. Palanisamy [a,*], N. Kalyanasundaram [b], P.M. Swetha [a]

[a] Department of Electronics and Communication Engineering, National Institute of Technology, Tiruchirappalli 620015, India
[b] Department of Electronics and Communication Engineering, Jaypee Institute of Information Technology, Noida 201307, India

ARTICLE INFO

Article history:
Received 21 October 2010
Received in revised form
6 April 2011
Accepted 31 May 2011
Available online 14 June 2011

Keywords:
Direction of arrival
Angle estimation
Cross-correlation
Coherent signal
Acoustic vector sensor array

ABSTRACT

In this paper, we present two new methods for estimating two-dimensional (2-D) direction-of-arrival (DOA) of narrowband coherent (or highly correlated) signals using an L-shaped array of acoustic vector sensors. We decorrelate the coherency of the signals and reconstruct the signal subspace using cross-correlation matrix, and then the ESPRIT and propagator methods are applied to estimate the azimuth and elevation angles. The ESPRIT technique is based on the shift invariance property of array geometry and the propagator method is based on partitioning of the cross-correlation matrix. The propagator method is computationally efficient and requires only linear operations. Moreover, it does not require any eigendecomposition or singular-value decomposition as for the ESPRIT method. These two techniques are direct methods which do not require any 2-D iterative search for estimating the azimuth and the elevation angles. Simulation results are presented to demonstrate the performance of the proposed methods.

1. Introduction

In recent years, acoustic vector sensor array processing has been drawing the increasing attention of the underwater signal processing community. An acoustic vector sensor measures both pressure and particle velocity of the acoustic field at a point in space whereas a traditional pressure sensor can only extract the pressure information. The main advantage of these vector sensors over traditional scalar sensors is that they make better use of the available acoustic information; hence they should outperform the scalar (pressure)-sensor arrays in terms of accuracy. Thus vector sensors should allow the use of smaller array apertures while maintaining performance.

Acoustic vector sensor model was first introduced to the signal processing community in Ref. [1]. Since then, many advanced pressure-sensor array techniques were adapted to the acoustic vector sensor array [2–4]. Various types of acoustic vector sensors with different design technologies are now commercially available [5]. Vector sensor technologies have been used in the field of underwater acoustics for decades and attract reinvigorated attention for underwater source location problems.

Most of the high-resolution DOA methods such as MUSIC [6,7] and ESPRIT [8,9] have been proven to be effective when the signals are uncorrelated. When the signal sources are coherent or highly correlated as occurs, for example, in multipath propagation or in military scenarios involving smart jammers, the performance of these techniques, however, degrades dramatically. Under this circumstance, the rank of the covariance matrix is generally less than the number of incident signals. To overcome this detrimental aspect, decorrelation techniques such as the spatial smoothing (SS) [10–12], the technique developed by Kozick and

* Corresponding author.
E-mail addresses: palan@nitt.edu (P. Palanisamy), n.kalyanasundaram@jiit.ac.in (N. Kalyanasundaram), 208108002@nitt.edu (P.M. Swetha).

0165-1684/$ - see front matter © 2011 Elsevier B.V. All rights reserved.
doi:10.1016/j.sigpro.2011.05.021

Kassam [13], eigenvector smoothing (ES) [14,15], and computationally efficient subspace-based method without eigendecomposition (SUMWE) [16] have been proposed. These techniques, however, work well only for certain array configurations, e.g., uniformly spaced linear arrays.

There has been growing interest in developing 2-D DOA estimators using 2-D array of sensors with simple structure, e.g., L-shaped arrays, for better estimation performance and without encountering the pair-matching problem. Tayem and Kwon [17] proposed a method for estimating 2-D DOA in the presence of uncorrelated or partially correlated signals exploiting the L-shaped array structure. Kikuchi et al. [18] developed an automatic pair-matching method for DOA estimation using the cross-correlation matrix. Although these methods work very well for uncorrelated signals, extension to the coherent signals in multipath-propagation scenarios requires further investigation. Gu et al. [19] developed an effective 2-D DOA estimation method for narrowband coherent signals using L-shaped arrays.

This paper aims to develop effective 2-D DOA estimation methods for narrowband coherent signals using an L-shaped acoustic vector sensor array. The proposed method using acoustic ESPRIT has the advantage of estimating the elevation and azimuth angles using a small number of sensor elements accurately. The proposed method using acoustic propagator estimates elevation and azimuth angles with reduced computational complexity. In the proposed method using acoustic ESPRIT, the coherent signals are first decorrelated and a signal subspace is reconstructed from the cross-correlation matrix of two sub-arrays. Then the shift invariance property can be employed to estimate the azimuth and elevation angles. We are using ESPIRIT invariance technique in particular for angle estimation. Proposed acoustic propagator method uses the propagator matrix obtained from the cross-correlation matrix to estimate the elevation and the azimuth angles.

The paper is organized as follows: In Section 2, the data model for an L-shaped acoustic vector sensor array is presented. Section 3, the proposed DOA algorithm using ESPRIT and propagator methods for coherent signals is derived. In Section 4, we present the numerical simulations that illustrate the root mean-square error (RMSE) reduction achieved by the proposed method as compared to the methods using only the pressure sensor array. Finally, Section 5 concludes the paper.

Throughout this paper, vectors are denoted by lowercase bold letters and matrices by uppercase bold letters. The superscripts T and H denote, respectively, transposition and conjugate transposition.

2. Acoustic vector sensor array data model

Consider an L-shaped acoustic vector sensor array consisting of two orthogonal uniform linear sub-arrays, one along z-direction and other along x-direction, employing $2(M+l-1)$, $l \in N$, sensor elements with interspacing d and with a common element at origin. The sub-array along the z-direction consists of $(M+l)$ sensor elements and that along the x-direction consists of $(M+l-1)$ sensor elements. The common element placed at the origin serving as the reference for both the linear sub-arrays. The first l sensor elements (counting the common reference sensor also) along the x-direction and the z-direction are considered as dummy elements and the remaining $(2M-1)$ sensors alone are considered to be functional. The purpose of $(2l-1)$ dummy elements is to ensure sufficient spatial separation between the two sub-arrays so that the noise at any two of the functional sensors belonging to the different sub-arrays can be considered to be spatially uncorrelated with negligible error.

Suppose that there are D narrowband plane wave signals, $s_i(t)$, $i=1, 2, \ldots, D$, with wavelength λ impinging on the acoustic vector sensor array from distinct directions at elevation angles θ_i, $i=1, 2, \ldots, D$ and azimuth angles φ_i, $i=1, 2, \ldots, D$, as shown in Fig. 1. Assume that these signals are in the far-field with respect to the array location. Each element of the acoustic vector array produces an output, which is a 4×1 vector, corresponding to the acoustic pressure and the acoustic particle velocity. In other words, each acoustic vector sensor is equivalent to four scalar sensors; three velocity-component sensors and one pressure sensor co-located in space. The 4×1 array manifold vector of the acoustic vector sensor [2] with respect to the ith signal is given by

$$\mathbf{c}(\theta_i,\varphi_i) \triangleq [\alpha_i\ \beta_i\ \gamma_i 1]^T \text{ for } i = 1,2,\ldots,D \tag{1}$$

where $\alpha_i = \sin\theta_i \cos\varphi_i$, $\beta_i = \sin\theta_i \sin\varphi_i$ and $\gamma_i = \cos\theta_i$ for $i=1, 2, \ldots, D$.

Therefore the received signal at each element of the acoustic vector sensor array will be a 4×1 vector given by

$$\mathbf{u}_m(t) = [u_{mv_1}(t)\ u_{mv_2}(t)\ u_{mv_3}(t)\ u_{mp}(t)]^T \tag{2}$$

where $u_{mv_j}(t)$ for $j=1,2,3$, and $u_{mp}(t)$ denotes, respectively, the jth velocity component and the acoustic pressure of the received signal at the mth element of the acoustic vector sensor array. In the sequel, the symbols $x(t)$ and $z(t)$ will be used, respectively, to represent the signal received

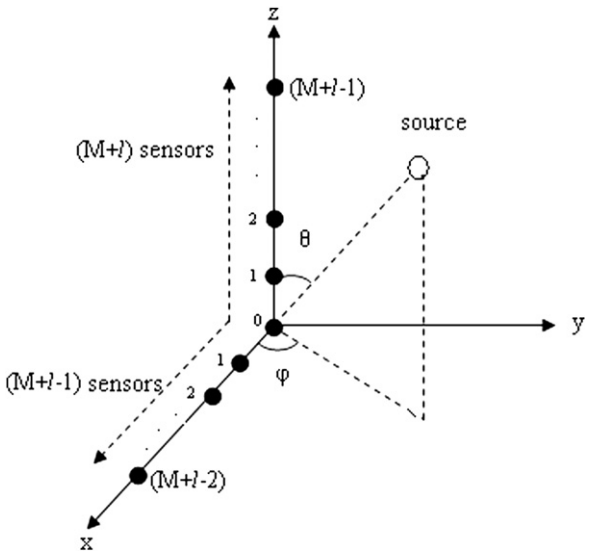

Fig. 1. Array geometry.

by the sub-arrays along the x-axis and the z-axis instead of $u(t)$.

Now the sampled version of the noise-corrupted 4×1 signal vector received at the mth functional sensor element of the acoustic vector sensor array along the x-axis can be expressed as

$$\mathbf{x}_m(t)=\sum_{i=1}^{D} s_i(t)e^{jm\psi_i}\,\mathbf{c}(\theta_i,\varphi_i)+\mathbf{n}_{xm}(t) \text{ for } m=l,\ l+1,\ \ldots,(M+l-2) \text{ and } t=1,\,2,\,\ldots,\,N \tag{3}$$

where $\psi_i=(2\pi d/\lambda)\alpha_i$ for $i=1,\ 2,\ldots,\ D$, $\mathbf{n}_{xm}(t)\triangleq[n_{xmv_1}(t)\ n_{xmv_2}(t)\ n_{xmv_3}(t)\ n_{xmp}(t)]^T$ is the 4×1 noise vector at the mth sensor of the acoustic vector sensor array along the x-axis, and $n_{xmv_j}(t)$ for $j=1,\ 2,\ 3$, and $n_{xmp}(t)$ denote, respectively, the jth velocity component and the pressure component of the noise vector at the mth element of the acoustic vector sensor array. The entire set of received samples at all the functional sensors (that is, from lth sensor to $(M+l-2)$th sensor) along the x-axis can be represented as

$$\mathbf{x}(t)=A_x\boldsymbol{\Phi}_x^l s(t)+\mathbf{n}_x(t) \text{ for } t=1,2,\ldots,N \tag{4}$$

where $\mathbf{x}(t)\triangleq[\mathbf{x}_l^T(t)\,\mathbf{x}_{l+1}^T(t)\ldots\mathbf{x}_{M+l-2}^T(t)]^T$ is the $4(M-1)\times 1$ observation vector (snap-shot vector) at the acoustic vector sensor array along the x-axis, $\mathbf{A}_x\triangleq[\boldsymbol{a}_x(\theta_1,\varphi_1)\boldsymbol{a}_x(\theta_2,\varphi_2)\ldots\boldsymbol{a}_x(\theta_D,\varphi_D)]$ is the $4(M-1)\times D$ array manifold matrix of the acoustic vector sensor array along the x-axis, $\Phi_x\triangleq diag\{e^{\psi y_1},\,e^{\psi y_2},\,\ldots,e^{\psi y_D}\}$ is a $D\times D$ diagonal matrix, $\mathbf{s}(t)\triangleq[s_1(t)s_2(t)\ldots s_D(t)]^T$ is the $D\times 1$ signal vector, $\mathbf{n}_x(t)\triangleq[\mathbf{n}_{xl}^T(t)\,\mathbf{n}_{x(l+1)}^T(t)\ldots\mathbf{n}_{x(M+l-2)}^T(t)]^T$ is the $4(M-1)\times 1$ noise vector at the acoustic vector sensor array along the x-axis and $\mathbf{a}_x(\theta_i,\varphi_i)\triangleq\mathbf{q}_x(\theta_i,\varphi_i)\otimes\mathbf{c}(\theta_i,\varphi_i)$ is the $4(M-1)\times 1$ array manifold vector of the acoustic vector sensor array along the x-axis and where the symbol '$\otimes$' denotes Kronecker product and $\mathbf{q}_x(\theta_i,\varphi_i)\triangleq[1e^{j\psi_i}e^{j2\psi_i}\ldots e^{j(M-2)\psi_i}]^T$ is the $(M-1)\times 1$ vector of inter-vector sensor spatial phase factors for the ith incident source signal along the x-axis.

In similar way, the received samples at all the functional sensors (that is, from lth sensor to $(M+l-1)$th sensor) along the z-axis can be represented as

$$\mathbf{z}(t)=A_z\boldsymbol{\Phi}_z^l s(t)+\mathbf{n}_z(t) \text{ for } t=1,2,\ldots,N \tag{5}$$

where $\mathbf{z}(t)\triangleq[\mathbf{z}_l^T(t)\,\mathbf{z}_{l+1}^T(t)\ldots\mathbf{z}_{M+l-1}^T(t)]^T$ is the $4M\times 1$ observation vector at the acoustic vector sensor array along the z-axis, $\mathbf{A}_z\triangleq[\boldsymbol{a}_z(\theta_1,\varphi_1)\,\boldsymbol{a}_z(\theta_2,\varphi_2)\ldots\boldsymbol{a}_z(\theta_D,\varphi_D)]$ is the $4M\times D$ array manifold matrix of the acoustic vector sensor array along the z-axis $\boldsymbol{\Phi}_z\triangleq$diag$\{e_1^{j\xi},\,e_2^{j\xi},\,\ldots,e_D^{j\xi}\}$ is a $D\times D$ diagonal matrix $\mathbf{n}_z(t)\triangleq[\mathbf{n}_{zl}^T(t)\,\mathbf{n}_{z(l+1)}^T(t)\ldots\mathbf{n}_{z(M+l-1)}^T(t)]^T$ is the $4M\times 1$ noise vector at the acoustic vector sensor array along the z-axis and $\boldsymbol{a}_z(\theta_i,\varphi_i)\triangleq\mathbf{q}_z(\theta_i)\otimes\mathbf{c}(\theta_i,\varphi_i)$ is the $4M\times 1$ array manifold vector of the acoustic vector sensor array along the z-axis and where $\mathbf{q}_z(\theta_i)\triangleq[1e^{j\xi_i}e^{j2\xi_i}\ldots e^{j(M-1)\xi_i}]^T$ is the $M\times 1$ vector of inter-vector sensor spatial phase factors for the ith incident source signal along the z-axis and $\xi_i=(2\pi d/\lambda)\gamma_i$.

For this problem we divide the number of source signals into 'p' groups such that the signals in the same group are coherent (i.e. the delayed and scaled replica of one other), but uncorrelated to the signals in the other groups. We assume that both the number of source signals D and the group number p are a'priori known with $M-D>L_{\max}$, where $L_{\max}\triangleq\max\{L_1,L_2,\ldots,L_p\}$ and L_k is the number of coherent signals in the kth group. Standard methods together with their many variants are already available in the literature [20–30] for estimating number of coherent source signals. Therefore, the number of source signals D and the group number p can be pre-estimated using one of the available techniques. Further, we assume that the components of the noise vectors $\mathbf{n}_{xk}(t)$ for $k=l,\ l+1,\ \ldots,\ (M+l-2)$ and $\mathbf{n}_{zm}(t)$ for $m=l,\ l+1,\ \ldots,\ (M+l-1)$, at various sensor outputs of the acoustic vector sensor array, are uncorrelated with the source signals $s_i(t)$ for $i=1,\,2,\ldots,\,D$ and, under the reasonable assumption that the spatial correlation between the noise processes at two different sensor locations falls off rapidly with increasing spatial separation, the noise vector $\mathbf{n}_{zm}(t)$ for $m=l,\ l+1,\ \ldots,\ (M+l-1)$, of the acoustic vector sensor array along the z-axis is uncorrelated with the noise vector $\mathbf{n}_{xk}(t)$ for $k=l,\ l+1,\ \ldots,\ (M+l-2)$, of the acoustic vector sensor array along the x-axis as long as l is not too small. Thus we have

$$E\{\mathbf{n}_{zm}(t)\mathbf{n}_{xk}^H(t)\}=\mathbf{0}_{4\times 4} \text{ for each } k=l,l+1,\ldots,(M+l-2) \text{ and } m=l,l+1,\ldots,(M+l-1) \tag{6}$$

where $\mathbf{0}_{4\times 4}$ is a 4×4 matrix with all entries equal to zero.

The problem is to estimate from the observations $\mathbf{x}(t)$ and $\mathbf{z}(t)$ for $t=1,\ 2,\ \ldots,\ N$, of the acoustic vector sensor arrays along x-axis and z-axis, where N denotes the number of snap-shots, the DOA parameters (θ_i,φ_i) for $i=1,\ 2,\ \ldots,\ D$ of the incident source signals. For this problem we shall work with the cross-correlation values computed between the observation vectors $\mathbf{z}(t)$ and $\mathbf{x}_m(t)$ for $m=l,\ l+1,\ \ldots,\ (M+l-2)$.

3. Proposed techniques for DOA estimation

The cross-correlation $\mathbf{r}_{zx_k}$ between the observation vectors $\mathbf{z}(t)$ and $\mathbf{x}_k(t)$ for each $k=l,\ l+1,\ \ldots,(M+l-2)$, is a $4M\times 4$ matrix defined as follows:

$$\mathbf{r}_{zx_k}\triangleq E\{\mathbf{z}(t)\mathbf{x}_k^H(t)\}=[\mathbf{r}_{z_lx_k}^T\,\mathbf{r}_{z_{l+1}x_k}^T\ldots\mathbf{r}_{z_{M+l-1}x_k}^T]^T \tag{7}$$

where $\mathbf{r}_{z_mx_k}^T\triangleq E[\mathbf{z}_m(t)\,\mathbf{x}_k^H(t)]$, for $m=l,\ l+1,\ \ldots,\ (M+l-1)$, is a 1×4 vector. For each $k=l,\ l+1,\ \ldots\ (M+l-2)$, the 4×1 received vector, $\mathbf{x}_k(t)$, in (2) can be expressed in matrix notation as

$$\mathbf{x}_k(t)=\mathbf{B}_{x_k}^H\mathbf{s}(t)+\mathbf{n}_{xk}(t) \tag{8}$$

where $\mathbf{B}_{xk}\triangleq[e^{-jk\psi_1}\mathbf{c}(\theta_1,\varphi_1)e^{-jk\psi_2}\mathbf{c}(\theta_2,\varphi_2)\ldots e^{-jk\psi_D}\mathbf{c}(\theta_D,\varphi_D)]^T$ is a $D\times 4$ matrix. Now, substituting (5) and (8) in (7) and using (6), we can write the expression for the cross-correlation as

$$\mathbf{r}_{zx_k}=\mathbf{A_z}\boldsymbol{\Phi}_z^l\mathbf{R}_s\mathbf{B}_{x_k} \text{ for } k=l,l+1,\ldots,(M+l-2) \tag{9}$$

where $\mathbf{R}_s\triangleq E[\mathbf{s}(t)\,\mathbf{s}^H(t)]$ is a $D\times D$ autocorrelation matrix of the signal. The cross-correlation matrix $\mathbf{R}_{zx}$, which is a $4M\times 4(M-1)$ matrix, is formed by concatenating $\mathbf{r}_{zx_k}$ for $k=l,\ l+1,\ \ldots,\ (M+l-2)$,as

$$\mathbf{R}_{zx}=[\mathbf{r}_{zx_l}\mathbf{r}_{zx_{l+1}}\ldots\mathbf{r}_{zx_{(M+l-2)}}] \tag{10}$$

By substituting (9) in (10), the expression for the cross-correlation matrix $\mathbf{R}_{zx}$ can be represented as

$$\mathbf{R}_{zx} = \mathbf{A_z}\mathbf{\Phi}_z^l\mathbf{R_s}\mathbf{\Phi}_x^l\mathbf{A}_x^H \tag{11}$$

If all the incident source signals are uncorrelated (i.e. incoherent), the number of groups will be equal to the number of source signals (i.e. $p=D$) and the rank $\{\mathbf{R}_s\}=p=D$. Then the rank of the cross-correlation matrix $\mathbf{R}_{zx}$ will be equal to D, the number of incident source signals. Hence, using the cross-correlation matrix $\mathbf{R}_{zx}$, one can determine D orthogonal vectors to form a signal subspace spanned by the columns of $\mathbf{A}_z$. If the sources are correlated, on the other hand, the number of groups will be less than the number of source signals (that is, $p<D$) and the rank $\{\mathbf{R}_s\}=p<D$. Under this condition, the rank of the cross-correlation matrix $\mathbf{R}_{zx}$ will also be less than the number D of source signals. Therefore, we cannot form a signal subspace directly using the cross-correlation matrix $\mathbf{R}_{zx}$.

In order to decorrelate the coherent (correlated) sources, the $4M\times 4(M-1)$ cross-correlation matrix $\mathbf{R}_{zx}$ is first partitioned into $L_{\max}$ submatrices each of dimension $4(M-L_{\max}+1)\times 4(M-1)$. The jth sub-matrix, denoted by $\mathbf{R}_{zx}^{(j)}$, is formed from the $4(j-1)+1$)th row to the $4(M-L_{\max}+j)$th row of $\mathbf{R}_{zx}$. Now, we form a new matrix $\mathbf{R}$ by concatenating these $L_{\max}$ submatrices as

$$\mathbf{R} = [\mathbf{R}_{zx}^{(1)}\mathbf{R}_{zx}^{(2)}\ldots\mathbf{R}_{zx}^{(L_{max})}] \tag{12}$$

The dimension of the matrix $\mathbf{R}$ is $4(M-L_{\max}+1)\times 4(M-1)L_{\max}$. Using (11) in (12), the matrix $\mathbf{R}$ can be expressed in the partitioned form as

$$\mathbf{R} = \mathbf{A}_z^{(4(M-L_{\max}+1))}[\mathbf{\Phi}_z^l\mathbf{R}_s\mathbf{\Phi}_x^l\mathbf{A}_x^H\ \ \mathbf{\Phi}_z^{l+1}\mathbf{R}_s\mathbf{\Phi}_x^l\mathbf{A}_x^H\ \ldots\ \mathbf{\Phi}_z^{l+L_{\max}-1}\mathbf{R}_s\mathbf{\Phi}_x^l\mathbf{A}_x^H] \tag{13}$$

where $\mathbf{A}_z^{(4(M-L_{\max}+1))}$ consists of the first $4(M-L_{\max}+1)$ rows of the array manifold matrix $\mathbf{A}_z$. If the rank of the matrix $\mathbf{R}$ is equal to the number of incident source signals D, then, by singular value decomposition (SVD) of $\mathbf{R}$, one can determine D orthogonal vectors to form the signal subspace which can be considered as the linear span of the columns of $\mathbf{A}_z^{(4(M-L_{\max}+1))}$. The proof of the equality $\text{rank}\{\mathbf{R}\}=D$ is given below

From (13)

$$\mathbf{R} = \mathbf{A}_z^{(4(M-L_{\max}+1))}\mathbf{\Omega}_z\mathbf{\Psi}_x \tag{14}$$

where $\mathbf{\Omega}_z\triangleq[\mathbf{\Phi}_z^l\ \mathbf{\Phi}_z^{l+1}\ldots\mathbf{\Phi}_z^{l+L_{\max}-1}]$ is a $1\times L_{\max}$ block matrix each block of which is a $D\times D$ diagonal matrix and $\mathbf{\Psi}_x$ is a $L_{\max}\times L_{\max}$ block diagonal matrix with each diagonal block equal to the $D\times 4(M-1)$ matrix $\mathbf{R}_s\mathbf{\Phi}_x^l\mathbf{A}_x^H$. Since each diagonal block of $\mathbf{\Omega}_z$ is a full rank $D\times D$ matrix, $\text{rank}\{\mathbf{\Omega}_z\}=D$ and

$$\begin{aligned}\text{rank}\{\mathbf{R}_s\mathbf{\Phi}_x^l\mathbf{A}_x^H\} &= \min(\text{rank}(\mathbf{R}_s),\ \text{rank}\{\mathbf{\Phi}_x^l\},\text{rank}\{\mathbf{A}_x^H\}\\ &= \min(p,D,D) = p(\text{since rank}(\mathbf{R}_s)=p\le D)\end{aligned} \tag{15}$$

Since $\mathbf{\Psi}_x$ is a $L_{\max}\times L_{\max}$ block diagonal matrix, the rank of $\mathbf{\Psi}_x$ will be equal to $L_{\max}$ times the rank of its diagonal block, that is

$$\text{rank}\{\mathbf{\Psi}_x\} = L_{\max}\text{rank}\{\mathbf{R}_s\mathbf{\Phi}_x^l\mathbf{A}_x^H\} = pL_{\max} \tag{16}$$

The number of source signals D, the number of groups p and the maximum number $L_{\max}$ of coherent signals will always satisfy the following inequality:

$$p \ge D/L_{\max} \tag{17}$$

with equality if and only if the number of coherent signals in all groups are equal (i.e., $L_1=L_2=\ldots=L_{\max}$). Therefore

$$\begin{aligned}\text{rank}(\mathbf{R}) &= \min(\text{rank}\{\mathbf{A}_z^{(4(M-L_{\max}+1))}\},\ \text{rank}\{\mathbf{\Omega}_z\},\ \text{rank}\{\mathbf{\Psi}_x\})\\ &= \min(D,D,pL_{\max}) = D(\text{using}(17))\end{aligned} \tag{18}$$

Thus, the $\text{rank}\{\mathbf{R}\}=D$ and the proof is complete.

In order to bring the velocity components and the pressure components of the acoustic vector sensors together it is necessary to transform the matrix $\mathbf{R}$ using the exchange matrix $\mathbf{J}$. For this purpose, we define a new transformed matrix $\tilde{\mathbf{R}}$ by

$$\tilde{\mathbf{R}} = \mathbf{J}^{\mathrm{T}}\mathbf{R} = \tilde{\mathbf{A}}_z\mathbf{\Omega}_z\mathbf{\Psi}_x \tag{19}$$

where

$$\tilde{\mathbf{A}}_z\triangleq\mathbf{J}^T\mathbf{A}_z^{(4(M-L_{\max}+1))} \tag{20}$$

and $\mathbf{J}=[\mathbf{J}_1\ \ \mathbf{J}_2\ \ \mathbf{J}_3\ \ \mathbf{J}_4]$, $\mathbf{J}_i\triangleq[\mathbf{e}_i\ \mathbf{e}_{i+4}\ \mathbf{e}_{i+8}\ldots\mathbf{e}_{i+4(M-L_{max})}]$ for $i=1,2,3,4$ and $\mathbf{e}_j$ is the $4(M-L_{\max}+1)\times 1$ unit vector whose jth component is 1 and all other components are zero. Since all the columns of $\mathbf{J}$ are orthogonal to one another, the rank of $\mathbf{J}$ is obviously equal to $4(M-L_{\max}+1)$. It is now straightforward to show that the rank of $\tilde{\mathbf{R}}$ is equal to D (using the condition $M-L_{\max}>D$). Thus, by a singular value decomposition of $\tilde{\mathbf{R}}$, it is now possible to determine D orthogonal vectors to form the signal subspace which can be considered as the linear span of the columns of $\mathbf{A}_z^{(4(M-L_{\max}+1))}$.

3.1. ESPRIT method

Let $\tilde{\mathbf{A}}_z$ be partitioned as follows:

$$\tilde{\mathbf{A}}_z = [\mathbf{A}_{z1}^H\ \mathbf{A}_{z2}^H\ \mathbf{A}_{z2}^H\ \mathbf{A}_{z4}^H]^H \tag{21}$$

where

$$\begin{aligned}&\mathbf{A}_{z4} = [\tilde{\mathbf{q}}_z(\theta_1)\tilde{\mathbf{q}}_z(\theta_2)\ldots\tilde{\mathbf{q}}_z(\theta_D)]\\ &\tilde{\mathbf{q}}_z(\theta_i)\triangleq[1e^{j\xi_i}e^{j2\xi_i}e^{j(M-L_{\max}+1))\xi_i}]^T\ \text{for}\ i=1,2,\ldots,D,\\ &\mathbf{A}_{zj} = \mathbf{A}_{z4}\mathbf{\Gamma}_j\ \text{for}\ j=1,2,3,\end{aligned} \tag{22}$$

and $\mathbf{\Gamma}_1=\text{diag}\{\alpha_1,\ \alpha_2,\ \ldots,\ \alpha_D\}$, $\mathbf{\Gamma}_2=\text{diag}\{\beta_1,\ \beta_2,\ \ldots,\ \beta_D\}$ and $\mathbf{\Gamma}_3=\text{diag}\{\gamma_1,\ \gamma_2,\ \ldots,\ \gamma_D\}$ are $D\times D$ diagonal matrices. The relation (22) implies that the generalized eigenvalues of the matrix pair $(\mathbf{A}_{zj},\mathbf{A}_{z4})$ for $j=1,2,3$, are precisely the jth direction cosine of the D signal directions, and the ith diagonal entry of $\mathbf{\Gamma}_j$ for $i=1,2,3$ comprises precisely the jth direction cosine of the ith source for $i=1,\ 2,\ \ldots,\ D$. Thus, if we obtain an estimate of elements of $\mathbf{\Gamma}_j$ for $j=1,2,3$, we can obtain an estimate (θ_i,φ_i) for $i=1,\ 2,\ \ldots,\ D$. The application of ESPRIT to the matrix pairs in (22) will yield the estimates of the directional cosines (i.e. diagonal elements of $\mathbf{\Gamma}_j$ for $j=1,2,3$). In fact, for real-time implementation, the ESPRIT algorithm can be applied in parallel to these matrix pairs.

As in subspace methods (like MUSIC and ESPRIT methods) for DOA estimation, the range of $\tilde{\mathbf{R}}$, which is a

$4(M-L_{\max}+1)$-dimensional space, can be decomposed into two orthogonal subspaces; one is a D-dimensional subspace, called signal subspace, which is spanned by the singular vectors corresponding to the D largest singular values and the other one is a complementary $[4(M-L_{\max}+1)-D]$-dimensional subspace called noise subspace. The signal subspace and the noise subspace can be determined by singular value decomposition (SVD) of the matrix $\tilde{\mathbf{R}}$. Let $\mathbf{U}_s$, called the signal-subspace matrix, be the $4(M-L_{\max}+1)\times D$ matrix composed of the singular vectors corresponding to the D largest singular values of $\tilde{\mathbf{R}}$. Then, the columns of $\tilde{\mathbf{A}}_z$ span the signal subspace. Therefore, the signal-subspace matrix $\mathbf{U}_s$ admits the decomposition

$$\mathbf{U}_s = \tilde{\mathbf{A}}_z \mathbf{T} \tag{23}$$

where $\mathbf{T}$ is a $D\times D$ non-singular matrix. The relation (23) implies that the singular vectors corresponding to the D largest singular values of the matrix $\tilde{\mathbf{R}}$ (i.e., the columns of $\mathbf{U}_s$) are linear combinations of the array manifold vectors of the D sources (i.e., the columns of $\tilde{\mathbf{A}}_z$).

Now, by substituting (21) in (23), the signal subspace matrix $\mathbf{U}_s$ can be partitioned as

$$\mathbf{U}_s = [\mathbf{U}_{s1}^H\ \mathbf{U}_{s2}^H\ \mathbf{U}_{s2}^H\ \mathbf{U}_{s4}^H]^H \tag{24}$$

where

$$\mathbf{U}_{sj} = \mathbf{A}_{zj}\mathbf{T} \text{ for j} = 1,2,3,4 \tag{25}$$

The relation $\mathbf{U}_{s4}=\mathbf{A}_{z4}\mathbf{T}$ implies that $\mathbf{A}_{z4}=\mathbf{U}_{s4}\mathbf{T}^{-1}$. Similarly $\mathbf{U}_{s1}=\mathbf{A}_{z1}\mathbf{T}=\mathbf{A}_{z4}\mathbf{\Gamma}_1\mathbf{T}$ (from (22)) implies $\mathbf{U}_{s1}=\mathbf{U}_{s4}\mathbf{T}^{-1}\mathbf{\Gamma}_1\mathbf{T}$. In similar way, we can write $\mathbf{U}_{s2}=\mathbf{U}_{s4}\mathbf{T}^{-1}\mathbf{\Gamma}_2\mathbf{T}$ and $\mathbf{U}_{s3}=\mathbf{U}_{s4}\mathbf{T}^{-1}\mathbf{\Gamma}_3\mathbf{T}$.

We define

$$\mathbf{\Lambda}_j = \mathbf{T}^{-1}\mathbf{\Gamma}_j\mathbf{T} \text{ for } j = 1,2,3 \tag{26}$$

Note that the eigenvalues of $\mathbf{\Lambda}_j$, $j=1, 2, 3$, are the diagonal elements of the matrix $\mathbf{\Gamma}_j$, $j=1,2,3$. Thus, if we can form an estimate of the matrix $\mathbf{\Lambda}_j$, $j=1, 2, 3$, and compute its eigenvalues, we can obtain an estimate of (θ_i, φ_i) for $i=1, 2, \ldots,$ D. In terms of the signal-subspace singular vectors, the relations $\mathbf{A}_{zj}=\mathbf{A}_{z4}\mathbf{\Gamma}_j$ for $j=1, 2, 3$, become

$$\mathbf{U}_{sj} = \mathbf{U}_{s4}\mathbf{\Lambda}_j \text{ for } j = 1,2,3 \tag{27}$$

The set of relations (27) is an overdetermined system of linear equations. In practice we do not know the signal subspace singular vectors and must estimate them from a finite number of observations. The cross-correlation vector $\mathbf{r}_{zx_k}$, defined in (7), has to be estimated by the corresponding time averaged cross-correlation vector $\hat{\mathbf{r}}_{zx_k}$ based on finite number of observations of the vectors $\mathbf{z}(t)$ and $\mathbf{x}_k(t)$ for $t=1, 2, \ldots, N$. The estimate $\hat{\mathbf{r}}_{zx_k}$ of the cross-correlation vector $\mathbf{r}_{zx_k}$ can be computed as

$$\hat{\mathbf{r}}_{zx_k} = \frac{1}{N}\sum_{t=1}^{N}\mathbf{z}(t)\mathbf{x}_k^H(t) \tag{28}$$

Then we can form the estimate $\hat{\tilde{\mathbf{R}}}$ of the matrix $\tilde{\mathbf{R}}$ using the estimate $\hat{\mathbf{r}}_{zx_k}$ of the cross-correlation vector. The singular vector corresponding to the D largest singular values of $\hat{\tilde{\mathbf{R}}}$ will be the estimate of the signal subspace singular vectors. Let us denote the estimates of $\mathbf{U}_{sj}$ and $\mathbf{\Lambda}_j$, respectively, by $\hat{\mathbf{U}}_{sj}$ and $\hat{\mathbf{\Lambda}}_j$. The relation $\mathbf{U}_{sj}=\mathbf{U}_{s4}\mathbf{\Lambda}_j$ for $j=1, 2, 3$, between the submatrices $\mathbf{U}_{sj}$ for $j=1, 2, 3$, and $\mathbf{U}_{s4}$ may not be satisfied exactly by the estimates of the signal subspace singular vectors. However, a least-squares solution of the overdetermined system of linear Eq. (27) for the matrix $\hat{\mathbf{\Lambda}}_j$ may be obtained by minimizing the cost functions

$$\varepsilon(\hat{\mathbf{\Lambda}}_j) = \|\hat{\mathbf{U}}_{sj} - \hat{\mathbf{U}}_{s4}\hat{\mathbf{\Lambda}}_j\|_F^2 \quad \text{for } j = 1,2,3,$$

where $\|\bullet\|_F$ denotes the Frobenius norm. The cost functions $\varepsilon(\hat{\mathbf{\Lambda}}_j)$for $j=1, 2, 3$, being quadratic (convex) functions of $\hat{\mathbf{\Lambda}}_j$, may be minimized to give the unique least-squares solution for $\hat{\mathbf{\Lambda}}_j$:

$$\hat{\mathbf{\Lambda}}_j = (\hat{\mathbf{U}}_{sj}\hat{\mathbf{U}}_{s4})^{-1}(\hat{\mathbf{U}}_{sj}^H\hat{\mathbf{U}}_{sj}) \text{ for } j = 1, 2, 3 \tag{29}$$

It is discussed in Refs. [31, and 32] that the maximum possible finite-sample accuracy may be achieved if (27) is solved for $\hat{\mathbf{\Lambda}}_j$ by a Total Least Square (TLS) method. Let us denote the eigenvalues of $\hat{\mathbf{\Lambda}}_j$ by $\lambda_1^{(j)}, \lambda_D^{(j)}, \ldots\lambda_D^{(j)}$ for $j=1, 2, 3$. From these, the values of α_i, β_i, and γ_i for $i=1, 2, \ldots, D$, may be estimated as

$$\hat{\alpha}_i = \lambda_i^{(1)},\ \hat{\beta}_i = \lambda_i^{(2)} \text{ and } \hat{\gamma}_i = \lambda_i^{(3)} \text{ for } i = 1,2,\ldots,D \tag{30}$$

Then, the estimates of the azimuth and the elevation angles for each source can be determined as

$$\hat{\phi}_i = \tan^{-1}(\hat{\beta}_i/\hat{\alpha}_i) \text{for } i = 1,2,\ldots,D \tag{31a}$$

$$\hat{\theta}_i = \tan^{-1}(\hat{\alpha}_i/\hat{\gamma}_i\cos\hat{\varphi}_i) \text{ for } i = 1,2,\ldots,D \tag{31b}$$

Note that the estimate $\hat{\theta}_i$, $i=1, 2, \ldots, D$, of the elevation angle θ_i, $i=1, 2, \ldots, D$, can be determined from (31b) using the estimate $\hat{\varphi}_i$ of the azimuth angle φ_I for $i=1, 2, \ldots, D$, in (31a). Both the elevation angle and azimuth angle estimates in (31a) and (31b) are using arc-tangent operation, which allows its argument value to be greater than unity. The arc-tangent operation is a one-to-one mapping for the range $(-\pi/2, \pi/2)$ and the domain $\Re$ of real numbers. That is, the arc-tangent value always exists for any real number and the method will never fail. This is also one of the main advantages of the proposed techniques over the methods in Refs. [2–4,9]. The methods in Refs. [2–4,9] use the arc-sine and arc-cosine operations for estimating the DOAs. These arc-sine and arc-cosine operations are one-to-one mappings only for the range $(-\pi/2, \pi/2)$ and the domain $[-1, 1]$. In real-time scenario the argument value could be greater than one even for very high SNR leading to estimation failure.

Further, this ESPRIT-based DOA estimation method can provide closed-form estimates of angles with automatic pair matching of the azimuth and the elevation angles, for which a'priori knowledge of incident source location is not required. But, multiple signal classification (MUSIC) [6] algorithm requires a two-dimensional peak search for D maxima of a highly non-linear objective function corresponding to D sources each characterized by two estimation parameters. For fast convergence, MUSIC requires good initial estimate of source location. However, without any a'priori of knowledge of source locations, getting initial estimate is not feasible. Thus, ESPRIT-based method is computationally more efficient than spectral

MUSIC or root MUSIC algorithms [6,34]. In MUSIC, there is a possibility of convergence to local maxima leading to estimation failure but in contrast the ESPRIT-based technique is free from such problems.

3.1.1. Summarized procedure for DOA estimation using ESPRIT technique

Step 1. Calculate the estimate $\hat{\mathbf{r}}_{zx_k}$ of the cross-correlation vector $\mathbf{r}_{zxk}$ using (28).
Step 2. Form the estimate of the matrix $\mathbf{R}$ in (12) and then construct the estimate $\hat{\tilde{\mathbf{R}}}$ of $\tilde{\mathbf{R}}$ in (19).
Step 3. Compute the D singular vectors corresponding to the D largest singular values of $\hat{\tilde{\mathbf{R}}}$ by SVD and form the estimate of the signal subspace $\mathbf{U}_s$.
Step 4. Partition $\mathbf{U}_s$ according to (24) to find $\mathbf{U}_{sj}$ for $j=1.2.3.4$, and obtain $\hat{\mathbf{\Lambda}}_j$ for j=1, 2, 3, using (29).
Step 5. Find the eigenvalues of $\hat{\mathbf{\Lambda}}_j$ for $j=1, 2, 3$, and find the DOA estimates using (31).

3.2. Propagator method

In this section, we apply propagator method [33], which is computationally less intensive than the ESPRIT-based method, to (19). We first give the definition of the propagator. The $D\times D$ sub-matrix $\mathbf{A}_1$ comprising the last D rows of the $(M-L_{\max}+1)\times D$ matrix $\mathbf{A}_{z4}$ is a full rank (non-singular) matrix because of the Vandermonde structure. Therefore, any one of the remaining $[(M-L_{\max}+1)-\mathrm{D}]$ rows of the matrix $\mathbf{A}_{z4}$ can be expressed as a linear combination of the last D rows. Denoting by $\mathbf{A}_2$ the $[(M-L_{\max}+1)-D]\times D$ sub-matrix (of $\mathbf{A}_{z4}$) comprising these remaining $[(M-L_{\max}+1)-D]$ rows, we can partition the matrix $\mathbf{A}_{z4}$ as

$$\mathbf{A}_{z4}=[\mathbf{A}_2^H\mathbf{A}_1^H]^H \tag{32}$$

Now, substituting (32) in (21) and using the fact that $\mathbf{A}_{zj}=\mathbf{A}_{z4}\mathbf{\Gamma}_j$ for $j=1, 2, 3$, we can partition the matrix $\tilde{\mathbf{A}}_z$ (see (20)) as

$$\tilde{\mathbf{A}}_z=[\mathbf{B}_2^H\mathbf{A}_1^H]^H \tag{33}$$

where

$$\mathbf{B}_2=[(\mathbf{A}_2\mathbf{\Gamma}_1)^{\mathrm{H}}(\mathbf{A}_1\mathbf{\Gamma}_1)^{\mathrm{H}}(\mathbf{A}_2\mathbf{\Gamma}_2)^{\mathrm{H}}(\mathbf{A}_1\mathbf{\Gamma}_2)^{\mathrm{H}}(\mathbf{A}_2\mathbf{\Gamma}_3)^{\mathrm{H}}(\mathbf{A}_1\mathbf{\Gamma}_3)^{\mathrm{H}}\mathbf{A}_2^{H}]^{\mathrm{H}}$$

Under the hypothesis that $\mathbf{A}_1$ is a $D\times D$ non-singular matrix, the first $[4(M-L_{\max}+1)-D]$ rows of $\tilde{\mathbf{A}}_z$ (that is, all the rows of $\mathbf{B}_2$) can be expressed as a linear combination of the last D rows of $\tilde{\mathbf{A}}_z$(that is, all the rows of $\mathbf{A}_1$) so that the matrix $\mathbf{B}_2$ can be written in the form

$$\mathbf{B}_2=\mathbf{P}^{\mathbf{H}}\mathbf{A}_1 \tag{34}$$

where $\mathbf{P}^H$ is the $[4(M-L_{\max}+1)-D]\times D$ matrix whose entries are coefficients of the linear combinations. The conjugate transpose $\mathbf{P}$ of $\mathbf{P}^{\mathrm{H}}$ is the $D\times[4(M-L_{\max}+1)-D]$ propagator matrix. Now, we can partition the propagator matrix as

$$\mathbf{P}^H=\mathbf{B}_2{\mathbf{A}_1}^{-1}=[\mathbf{P}_1^H\mathbf{P}_2^H\mathbf{P}_3^H\mathbf{P}_4^H\mathbf{P}_5^H\mathbf{P}_6^H\mathbf{P}_7^H]^H \tag{35}$$

where

$$\mathrm{P}_1=\mathbf{A}_2\mathbf{\Gamma}_1\mathbf{A}_1^{-1} \tag{36}$$

$$\mathrm{P}_2=\mathbf{A}_1\mathbf{\Gamma}_1{\mathbf{A}_1}^{-1} \tag{37}$$

$$\mathrm{P}_3=\mathbf{A}_2\mathbf{\Gamma}_2{\mathbf{A}_1}^{-1} \tag{38}$$

$$\mathrm{P}_4=\mathbf{A}_1\mathbf{\Gamma}_2{\mathbf{A}_1}^{-1} \tag{39}$$

$$\mathrm{P}_5=\mathbf{A}_2\mathbf{\Gamma}_3{\mathbf{A}_1}^{-1} \tag{40}$$

$$\mathrm{P}_6=\mathbf{A}_1\mathit{\Gamma}_3{\mathbf{A}_1}^{-1} \tag{41}$$

$$\mathrm{P}_7=\mathbf{A}_2{\mathbf{A}_1}^{-1} \tag{42}$$

Eqs. (37), (39) and (41) imply that the diagonal entries of the matrices $\mathbf{\Gamma}_1$, $\mathbf{\Gamma}_2$ and $\mathbf{\Gamma}_3$ can be determined, respectively, by finding the D eigenvalues of the matrices $\mathbf{P}_2$, $\mathbf{P}_4$ and $\mathbf{P}_6$. Alternatively, the matrices $\mathbf{\Gamma}_1$, $\mathbf{\Gamma}_2$ and $\mathbf{\Gamma}_3$ can be obtained in another way from (36), (38) and (40) with the help of (42) in the following manner: From (42), we have

$$\mathbf{A}_2=\mathbf{P}_7\mathbf{A}_1 \tag{43}$$

Substitution of (43) into (36), (38) and (40) yields

$$\mathbf{P}_7^{\#}\mathbf{P}_1=\mathbf{A}_1\mathbf{\Gamma}_1{\mathbf{A}_1}^{-1} \tag{44}$$

$$\mathbf{P}_7^{\#}\mathbf{P}_3=\mathbf{A}_1\mathbf{\Gamma}_2{\mathbf{A}_1}^{-1} \tag{45}$$

$$\mathbf{P}_7^{\#}\mathbf{P}_5=\mathbf{A}_1\mathbf{\Gamma}_3{\mathbf{A}_1}^{-1} \tag{46}$$

where # denotes the pseudoinverse. Thus the diagonal elements of $\mathbf{\Gamma}_1$, $\mathbf{\Gamma}_2$ and $\mathbf{\Gamma}_3$ can also be determined, respectively, by finding the D eigenvalues of $\mathbf{P}_7^{\#}\mathbf{P}_1$, $\mathbf{P}_7^{\#}\mathbf{P}_3$ and $\mathbf{P}_7^{\#}\mathbf{P}_5$. The propagator matrix $\mathbf{P}$ may be obtained from the partition of the matrix $\tilde{\mathbf{R}}$

$$\tilde{\mathbf{R}}=[\mathbf{R}_2^H\mathbf{R}_1^H]^H \tag{47}$$

where $\mathbf{R}_1=\mathbf{A}_1\mathbf{\Omega}_z\mathbf{\Psi}_x$ and $\mathbf{R}_2=\mathbf{P}^H\mathbf{R}_1$. The relation $\mathbf{R}_2=\mathbf{P}^H\mathbf{R}_1$ between the submatrices $\mathbf{R_1}$ and $\mathbf{R}_2$ may not be satisfied in practice since the matrix $\hat{\tilde{\mathbf{R}}}$ must be estimated from a finite number of observation samples as discussed in the previous Section. However, by partitioning the estimate $\hat{\tilde{\mathbf{R}}}$ of the matrix $\tilde{\mathbf{R}}$ as in (47), the estimate $\hat{\mathbf{P}}$ of the propagator matrix $\mathbf{P}$ can be obtained by minimizing the cost function

$$\zeta(\hat{\mathbf{P}}^H)=\|\mathbf{R}_2-\hat{\mathbf{P}}^H\mathbf{R}_1\|_F^2$$

The cost function $\zeta(\hat{\mathbf{P}}^H)$, which is a quadratic (convex) function of $\hat{\mathbf{P}}^H$, may be minimized to give the unique least-square solution for $\hat{\mathbf{P}}^H$

$$\hat{\mathbf{P}}^H=\mathbf{R}_2\mathbf{R}_1^H(\mathbf{R}_1\mathbf{R}_1^H)^{-1} \tag{48}$$

Thus, the estimate $\hat{\mathbf{P}}$ of the propagator matrix $\mathbf{P}$ is obtained from the estimate $\hat{\tilde{\mathbf{R}}}$ of the matrix $\tilde{\mathbf{R}}$. Then, we can partition $\hat{\mathbf{P}}^H$ according to (35) to obtain the estimate $\hat{\mathbf{P}}_i$ of $\mathbf{P}_i$ for $i=1, 2, \ldots, 7$. Using these estimated matrices $\hat{\mathbf{P}}_i$ for $i=1, 2, \ldots,7$, we can obtain the estimate $\hat{\mathbf{\Gamma}}_j$ of the matrix $\mathbf{\Gamma}_j$ for $j=1, 2, 3$ and hence the values of α_i, β_i, and γ_i for $i=1, 2, \ldots, D$, may be estimated as

$$\hat{\alpha}_i=[\hat{\mathbf{\Gamma}}_1]_{ii},\quad \hat{\beta}_i=[\hat{\mathbf{\Gamma}}_2]_{ii} \text{ and } \hat{\gamma}_i=[\hat{\mathbf{\Gamma}}_3]_{ii} \text{ for } i=1, 2, \ldots, D \tag{49}$$

where $[\hat{\mathbf{\Gamma}}_j]_{ii}$ denotes the ith diagonal element $\hat{\mathbf{\Gamma}}_j$ for $j=1$,

2, 3. Then the DOA of the sources can be obtained using (31a) and (31b).

This propagator-based method can also provide closed form estimates of DOA parameters with automatic pair matching of the azimuth and the elevation angles like the ESPRIT-based technique. The propagator method requires only linear matrix operations. So, this method does not require any two-dimensional peak search and any eigen-decomposition or singular-value decomposition of the matrix $\mathbf{R}$ or $\tilde{\mathbf{R}}$ to form the signal subspace and the noise subspace. Therefore, the computational complexity of this method is less compared to the ESPRIT-based method or any other subspace-based DOA estimation methods, at the expense of a slight degradation in performance.

3.2.1. Summarized procedure for DOA estimation using propagator technique:

Step 1: Form the estimate $\hat{\tilde{\mathbf{R}}}$ of $\tilde{\mathbf{R}}$ as in the previous Section.
Step 2: Partition the matrix $\hat{\tilde{\mathbf{R}}}$ into two matrices $\mathbf{R}_1$ and $\mathbf{R}_2$ according to (47).
Step 4: Obtain the estimate $\hat{\mathbf{P}}$ of the propagator matrix $\mathbf{P}$ using (48).
Step 5: Partition $\hat{\mathbf{P}}^H$ according to (35) to find the estimate $\hat{\mathbf{P}}_i$ of $\mathbf{P}_i$ for $i=1, 2, \ldots, 7$.
Step 6: Find the eigenvalues of $\hat{\mathbf{P}}_7^{\#}\hat{\mathbf{P}}_1$, $\hat{\mathbf{P}}_7^{\#}\hat{\mathbf{P}}_3$ and $\hat{\mathbf{P}}_7^{\#}\hat{\mathbf{P}}_5$ and obtain the estimate $\hat{\mathbf{\Gamma}}_j$ of the matrix $\mathbf{\Gamma}_j$ for $j=1, 2, 3$.
Step 7: Find the DOA estimates using (31).

4. Simulations and results

In this section, simulation results are presented to demonstrate the effectiveness of the proposed methods in the 2-D DOA estimation of coherent signals using acoustic vector sensor array. We investigate the performance of the ESPRIT and the propagator methods in terms of the root mean square error (RMSE) of the DOA estimate as performance measure. In all the simulations, an L-shaped acoustic vector sensor array consisting of two orthogonal uniform linear sub-arrays, one along z-direction and other along x-direction, employing $2(M+l-1)$ sensor elements with same inter-element spacing and with the common element at origin is considered for the choice $l=1$. That is, the sensor at the origin (reference element) is considered as dummy element and the remaining $(2M-1)$ sensors (M sensors along z-direction and $(M-1)$ sensors along x-direction) are considered as functional. All the results presented here are obtained on the basis of 500 independent trials in the presence of zero-mean additive Gaussian noise with equal variance for all the sensors. The RMSE is defined [1] as

$$\text{RMSE} = \sqrt{\frac{1}{L}\sum_{k=1}^{L}\delta_k^2}$$

where L is the number independent trials and δ_k is the angular error for the kth trial. The angular error is defined as

$$\delta_k = 2\sin^{-1}\left(\frac{1}{2}\sqrt{(\hat{\alpha}_k-\alpha)^2+(\hat{\beta}_k-\beta)^2+(\hat{\gamma}_k-\gamma)^2}\right)$$

where $\hat{\alpha}_k = \sin\hat{\theta}_k\cos\hat{\phi}_k$, $\hat{\beta}_k = \sin\hat{\theta}_k\sin\hat{\phi}_k$ and $\hat{\gamma}_k = \cos\hat{\theta}_k$ are, respectively, the estimates of α, β and γ for the kth trial and where $(\hat{\theta}_k,\hat{\varphi}_k)$ is the DOA estimate corresponding to the actual direction (θ,φ) for the kth trial.

In the first experiment, we consider two coherent signals (that is, $D=2$, $p=1$, $L_1=2$ and $L_{\max}=2$) with identical powers and different DOAs $(\theta,\varphi)=(50^\circ, 60^\circ)$ and $(65^\circ, 70^\circ)$. The array consists of 12 sensors (that is, one dummy sensor at the origin, 6 functional sensors along z-direction and 5 functional sensors along x-direction) and 500 snap-shots are used. The RMSE for both the ESPRIT and the propagator-based techniques are computed for various signal-to-noise ratios (SNRs). The RMSE values for the signal 1 and signal 2 are, respectively, plotted in Figs. 2 and 3 as a function of SNR for both the ESPRIT and the propagator methods and are compared with the results of the methods proposed in [19] using only pressure sensors. For the second case, the above experiment is repeated for different snapshots at a fixed SNR of 10 dB and the corresponding RMSE values for source 1 and source 2 are plotted, respectively, in Figs. 4 and 5.

In the third test, we consider three narrowband signals of DOAs $(\theta,\varphi)=(50^\circ,40^\circ)$, $(60^\circ,50^\circ)$ and $(70^\circ,60^\circ)$, second and third signals being coherent and the first is uncorrelated with the second and the third signals. (i.e., $D=3$, $p=2$, $L_1=2$, $L_2=1$ and $L_{\max}=2$). The array consists of 16 sensors (that is, one dummy sensor at the origin, 8 functional sensors along z-direction and 7 functional sensors along x-direction) and 500 snap-shots are considered. Here the RMSE for both the ESPRIT and the propagator-based techniques are computed for various signal-to-noise ratios (SNRs). The RMSE values for signal 1, signal 2 and signal 3 are plotted, respectively, in Figs. 6–8 as a function of SNR for both the ESPRIT and the propagator methods and are compared with the results of the methods proposed in [19]. Results show that proposed acoustic ESPRIT method gives better RMSE performance compared to the pressure ESPRIT methods (Forward and

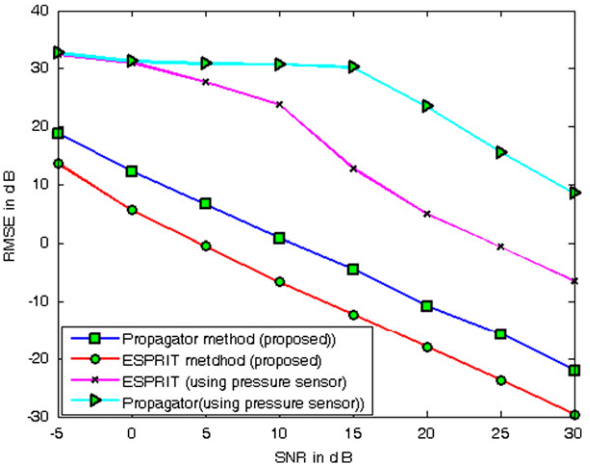

Fig. 2. RMSE for 2 coherent signals versus SNR for signal 1 at (50°, 60°).

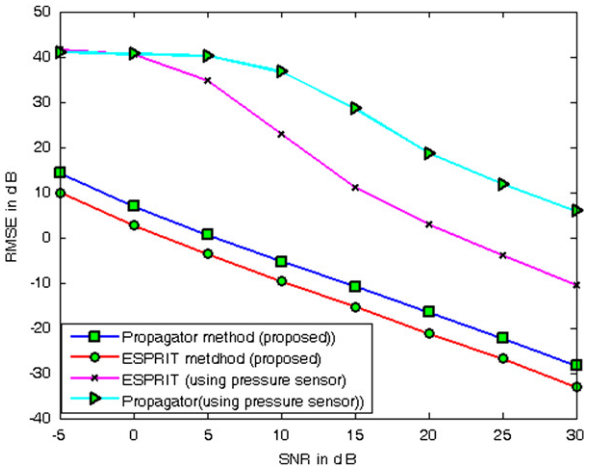

Fig. 3. RMSE for 2 coherent signals versus SNR for signal 2 at (65°, 70°).

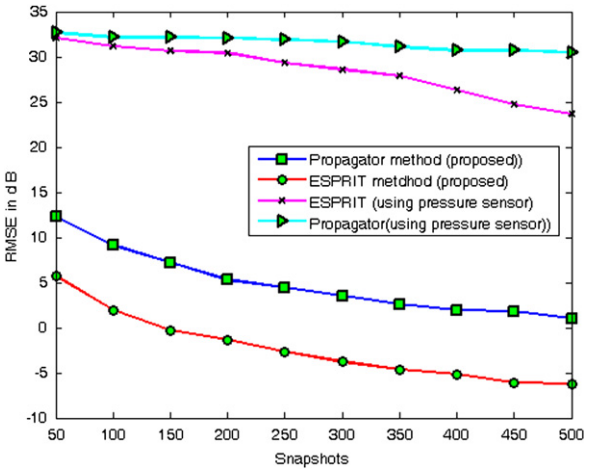

Fig. 4. RMSE for 2 coherent signals versus Snapshots for signal 1 at (50°, 60°).

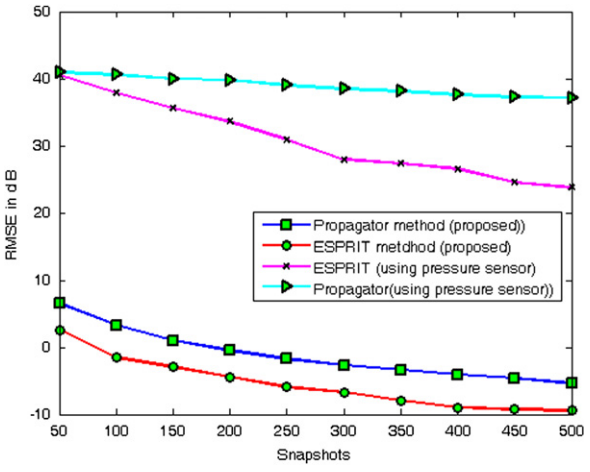

Fig. 5. RMSE for 2 coherent signals versus Snapshots for signal 2 at (65°, 70°).

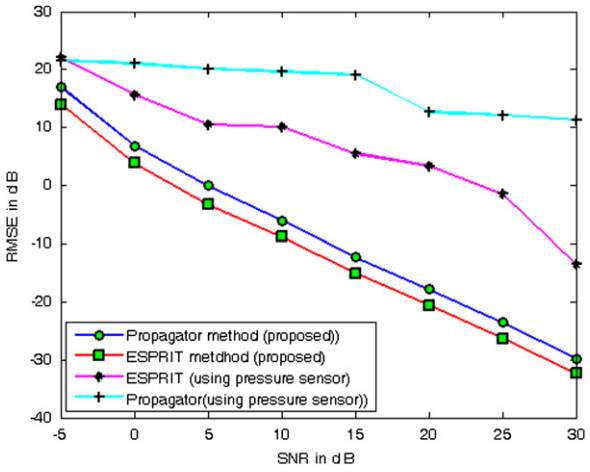

Fig. 6. RMSE for 3 signals (two coherent signals and one uncorrelated signal) versus SNR.

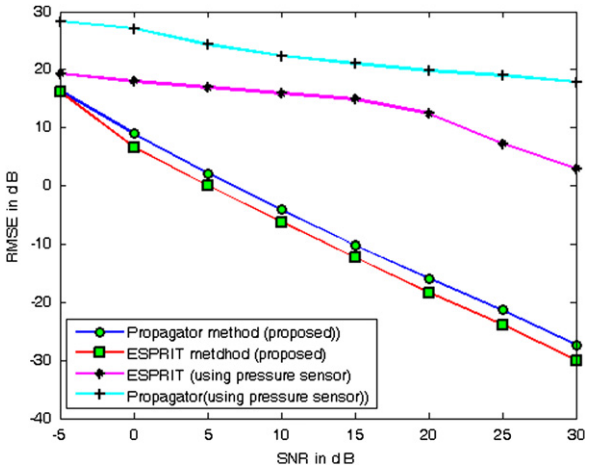

Fig. 7. RMSE for 3 signals (two coherent signals and one uncorrelated signal) versus SNR.

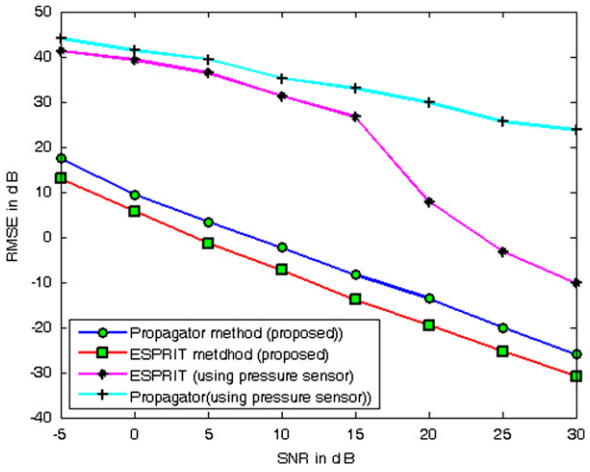

Fig. 8. RMSE for 3 signals (two coherent signals and one uncorrelated signal) versus SNR.

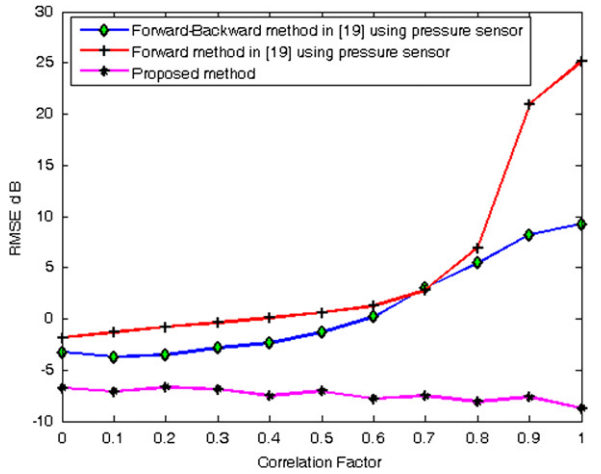

Fig. 9. RMSE for 2 coherent signals versus SNR for signal 1 at (50°, 40°).

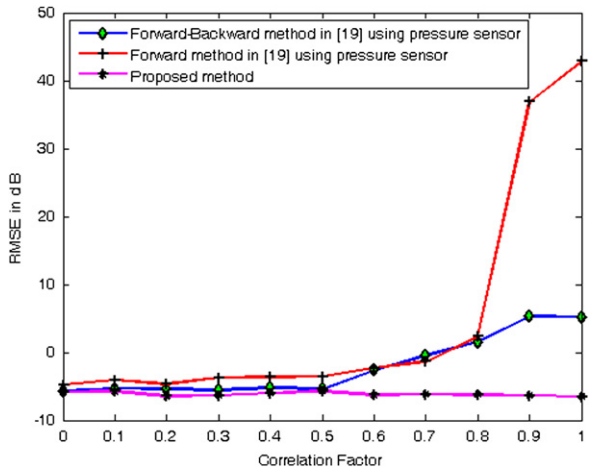

Fig. 10. RMSE for 2 coherent signals versus SNR for signal 1 at (60°, 50°).

FB). RMSE is found to be the least for the proposed acoustic ESPRIT method.

In the fourth test, we evaluate the performance of the proposed algorithm by varying the correlation between the signals at a fixed SNR. Here we consider two signals of DOAs (50°, 40°) and (60°, 50°). The number of sensors is 12 (that is, one dummy sensor at the origin, 6 functional sensors along *z*-direction and 5 functional sensors along *x*-direction). The correlation between the signals is varied from 0 to 1. The SNR is 10 dB and the number of snapshots is 500. Figs. 9 and 10 show the RMSE plots for the joint elevation and azimuth DOA estimation versus the correlation factor. From the plots it can be concluded that proposed acoustic ESPRIT gives better RMSE performance compared to pressure ESPRIT methods, especially when the correlation between the signals is high. Also the RMSE is seen to remain almost constant for the proposed acoustic ESPRIT method as the correlation between the signals is varied.

5. Conclusion

In this paper, we have presented two new methods based on ESPRIT and propagator techniques for estimating 2-D DOA of narrowband coherent sources using acoustic sensor array. Here we constructed a full rank cross-correlation matrix by decorrelating the coherency of the sources. The proposed techniques offer closed form automatically paired DOA estimation, which does not require any iterative peak search for estimating DOA parameters. The propagator-based technique requires less computation than the ESPRIT technique because the propagator method requires only linear matrix operations but no singular value decomposition. We conclude with the observation that the proposed acoustic sensor method, in contrast to the pressure sensor method, permits a further improvement in the quality of the DOA estimate by array aperture extension.

References

[1] A. Nehorai, E. Paldi, Acoustic vector-sensor array processing, IEEE Transactions on Signal Processing 42 (1994) 2481–2491.
[2] K.T. Wong, M.D. Zoltowski, Closed-form underwater acoustic direction-finding with arbitrarily spaced vector hydrophones at unknown locations, IEEE Journal of Oceanic Engineering 22 (1997) 566–575.
[3] J. He, Z. Liu, Two-dimensional direction finding of acoustic sources by a vector sensor array using the propagator method, Signal Processing 88 (2008) 2492–2499.
[4] J. He, Z. Liu, Efficient underwater two-dimensional coherent source localization with linear vector-hydrophone array, Signal Processing 89 (2009) 1715–1722.
[5] C.L. LeBlanc, Handbook of hydrophone element design technology, Naval Underwater Systems Center Tech. Rep., 1978, pp. 5813.
[6] R. Schmidt, Multiple emitter location and signal parameter estimation, IEEE Transactions on Antennas Propagation 34 (1986) 276–280.
[7] G. Bienvenu, L. Kopp, Optimality of high resolution array processing using the eigensystem approach, IEEE Transactions on Acoustics, Speech and Signal Processing 31 (1983) 1234–1248.
[8] R. Roy, T. Kailath, ESPRIT—Estimation of signal parameters via rotational invariance techniques, IEEE Transactions on Acoustics, Speech and Signal Processing 37 (1989) 984–995.
[9] M.D. Zoltowski, M. Haardt, C.P. Mathews, Closed-form 2-D angle estimation with rectangular arrays in element space of beamspace via unitary ESPRIT, IEEE Transactions on Signal Processing 44 (1996) 316–328.
[10] S.U. Pillai, B.H. Kwon, Forward/backward spatial smoothing techniques for coherent signal identification, IEEE Transactions on Acoustics, Speech and Signal Processing 37 (1989) 8–15.
[11] T.J. Shan, M. Wax, T. Kailath, On spatial smoothing for estimation of coherent signals, IEEE Transactions on Acoustics, Speech and Signal Processing 33 (1985) 806–811.
[12] J. Li, Improved angular resolution for spatial smoothing Techniques, IEEE Transactions on Signal Processing 40 (1992) 3078–3081.
[13] R.J. Kozick, S.A. Kassam, A unified approach to coherent source decorrelation by autocorrelation matrix smoothing, Signal Processing 45 (1995) 115–130.
[14] S.S. Reddi, A.B. Gershman, An alternative approach to coherent source location problem, Signal Processing 59 (1997) 221–233.
[15] D. Grenier, E. Bosse, A new spatial smoothing scheme for direction-of-arrivals of correlated sources, Signal Processing 54 (1996) 153–160.
[16] J. Xin, A. Sano, Computationally efficient subspace-based method for direction-of-arrival estimation without eigen decomposition, IEEE Transactions on Signal Process 52 (2004) 876–893.
[17] N. Tayem, H.M. Kwon, L-shape 2-dimensional arrival angle estimation with propagator method, IEEE Transactions on Antennas and Propagation 53 (2005) 1622–1630.
[18] S. Kikuchi, H. Tsuji, A. Sano, Pair-matching method for estimating 2-d angle of arrival with a cross-correlation matrix, IEEE Antennas and Wireless Propagation Letters 5 (2006) 35–40.

[19] J.F. Gu, P. Wei, H.M. Tai, 2-D direction-of-arrival estimation of coherent signals using cross-correlation matrix, Signal Processing 88 (2008) 75–85.
[20] M. Wax, I. Ziskind, Detection of the number of coherent signals by the MDL principle, IEEE Transactions on Acoustics, Speech and Signal Processing 37 (1989) 1190–1196.
[21] K. Minamisono, T. Shiokawa, Prediction of the number of coherent signals for mobile communicatin systems using autoregressive modeling, Electronics and Communications in Japan (Part-1: Communications) 77 (1994) 71–79.
[22] K. Huang, Z. Huang, Y. Zhou, Determining the number of coherent signal based on covariance matrix transforming, Signal Processing 19 (2003) 390–394.
[23] M. Tsuji, K. Umebayashi, Y. Kamiya, Y. Suzuki, A study on the accurate estimation of the number of weak coherent signals, in: Proceedings of the Sixth European Radar Conference, Rome, Italy, October-2009, pp. 234–237.
[24] J. Zhen, X. Si, L. Liu, Method for determining number of coherent signals in the presence of colored noise, Journal of Systems Engineering and Electronics 21 (2010) 297–30.
[25] M. Viberg, B. Ottersten, T. Kailath, Detection and estimation in sensor arrays using weighted subspace fitting, IEEE Transactions on Signal Processing 39 (1991) 2436–2449.
[26] M. Wax, T. Kailath, Detection of signals by information theoretic criteria, IEEE Transactions on Acoustics, Speech and Signal Processing 33 (1985) 387–392.
[27] E. Fishler, M. Grosmann, H. Messer, Detection of signals by information theoretic criteria: general asymptotic performance analysis, IEEE Transactions on Signal Processing 50 (2002) 1027–1036.
[28] J. Xin, N. Zheng, A. Sano, On-line detection of the number of narrowband signals with a Uniform Linear Array, in: Proceedings of the 16th European Signal Processing Conference (EUSIPCO 2008), Lausanne, Switzerland, August-2008, pp. 25–29.
[29] A.K. Seghouane, Multivariate regression model selection from small samples using Kullback's symmetric divergence, Signal Processing 86 (2006) 2074–2084.
[30] Y. Wu, K.W. Tam, On determination of the number of signals, in: Proceedings of the International Conference on Signal and Image Process, Honolulu, Hawai, August-2001, pp. 113–117.
[31] M. Viberg, B. Ottersten, Sensor array processing based on subspace fitting, IEEE Transactions on Signal Processing 39 (1991) 1110–1121.
[32] B. Ottersten, M. Viberg, T. Kailath, Performance analysis of the total least squares ESPRIT algorithm, IEEE Transactions on Signal Processing 39 (1991) 1122–1135.
[33] S. Marcos, A. Marsal, M. Benidir, The propagator method for source bearing estimation, Signal Processing 42 (1994) 121–138.
[34] K.T. Wong, M.D. Zoltowski, Root-MUSIC-based azimuth-elevation angle-of-arrival estimation with uniformly spaced but arbitrarily oriented velocity hrdrophones, IEEE Transactions on Signal Processing 47 (1999) 3250–3260.